LIQIONG ZHONG
YILONG LIANG
and
HAO HU

Deformation layer characteristics of ultrasonic deep rolling processing (UDRP), laser shot peening (LSP) and shot peening (SP) for Inconel718 super-alloy

This paper, by applying the ultrasonic deep rolling processing (UDRP), laser shot peening (LSP) and shot peening (SP) for Inconel718 super-alloy, adopts the laser confocal scanning microscope (LCSM) to observe surface topography and measure surface roughness, EBSD to observe the microscopic feature of surface hardened deformation layer, and x-ray stress analyzer and ultra-micro dynamic microhardness tester to measure residual stress and distribution of microhardness. The results show that, with the adopted surface hardening process parameters, the surface roughness presents in the order UDRP<without shot peening(WS)<LSP<SP; low-angle boundary on LSP surface is highly densified, but with shallower deformation layer, and the strain degree in microscell gradually decreases, with deeper strain layer for SP and UDRP, but unevenly; the maximum residual compressive stress of the three surface hardening methods are all applied on the surface with surface residual compressive stress LSP ≈ SP>UDRP and the layer depth of residual compressive stress UDRP>SP>LSP; surface microhardness LSP>SP>UDRP, and hardening depth SP ≈ UDRP>LSP.

Keywords: *Inconel718 super-alloy, ultrasonic deep rolling processing (UDRP), laser shot peening (LSP), shot peening (SP).*

1. Introduction

Inconel718 was Ni-Cr-Fe based precipitation hardening (PH) deformation super-alloy invented by American scientists in the 1950s. In 1968, it was modelled in China as GH4169 according to Chinese numbering method. Due to its high strength at below 650^{o}C and other outstanding performance such as good anti-fatigue, radio-resistance, antioxidant and anti-corrosion etc., this super-alloy has been widely applied in the aero-engine turbine disk, ring connector, vane and faster etc[1], for these aero-components requires the material to be of not only good strength and creep property, but also reliable fatigue.

Surface hardening is to form plastic deformation layer on metal surface and lead in residual compressive force to improve its fatigue performance. About the shot peening of Inconel718 super-alloy, the research of Tang Zhiguo et al.[2] showed that the residual compressive stress field of Imconel718 super-alloy shot peening was distributed in the "√" form, with maximum residual compressive stress 790MPa; SongYinggang et al.[3] revealed that in the interaction between twin crystal and dislocation, 1.2mm elastoplastic deformation was formed after GH4169 alloy shot peening; Wang Xin et al.[4] in their study indicated that the high-temperature low-cycle fatigue increased with the low-intensity shot peening for GH4169 pore structure, while the fatigue declined with the increased layer depth of residual compressive stress field after the high-intensity shot peening. In terms of the high-energy shot peening (HESP) of Inconel718 alloy, Feng Shuai et. al. found that GH4169 alloy could realize surface nanocrystallization after HESP[5-7], then present good performance of anti-high temperature oxidation in the air environment[8-9]; in the contrastive study of the surface structure between high-energy dry shot peening and wet shot peening, Cheng Shiping[10] found that the wet high-energy shot peening could gain not only better surface quality but also higher surface residual compressive stress than dry shot peening. In terms of the ultrasonic shot peening (USSP) of Inconel718 alloy, the study of Spanish scholar, Sandá[11] showed, the residual compressive stress and shot mark coverage could be increased by adding shot peening time, reduce the distance and shot quantity, but not finding the surface nanocrystallization. About the LSP of Inconel18, Pan Yinghui[12] and Teng Haishan[13] analyzed the residual compressive stress field of LSP by adopting ABAQUS and

Messrs. Liqiong Zhong, College of Mechanical Engineering, Guizhou University, Guiyang 550 025, Liqiong Zhong and Hao Hu, College of Mechanical Engineering, Guiyang University, Guiyang 550 005, Liqiong Zhong and Yilong Liang, Guizhou Key Laboratory of Materials Strength and Structure, Guizhou University, Guiyang 550 025 and Yilong Liang, High Performance Metal Structure Material and Manufacture Technology, National Local Joint Engineering Laboratory, Guiyang 550 025, China. E-mail: 1 zhenyuan04@163.com. Corresponding author: Yilong Liang, e-mail: liang_yilong@126.com

Ansys infinite element analysis method respectively, and indicated that the residual compressive stress level could be enhanced with the increased laser shocks[12]; the research of Zhou Jianzhong et al.[14] showed that the residual compressive stress of laser warm shot peening decreased gradually with the temperature increasing, but at 260ºC, the laser warm shot peeing was of better high-temperature stability; and the high-temperature releasing of surface hardening residual compressive stress meets the equation of Zener-Wert-Avrami[2,15]. About the UDRP of Inconel718 alloy, Doo[16] and Kim[17] conducted related research, finding that with UDRP, the rotating bending fatigue and friction wear property could be improved by the decreased surface roughness, surface structure hardening and residual compressive stress. He Jin[18] indicated in his study that the static pressure of UDRP had greatest influence on the high cycle fatigue of Inconel718 alloy, then the feed rate had the less influence, and the rotation had least influence. In the literature above about the surface hardening of Inconel718 alloy, their researches were made on the same type of surface hardening, but few have been on the comparison between different types of surface hardening for Inconel718 alloy[19].

Based on UDRP, LSP, SP for Inconel718, this paper compares the surface morphology, microstructure, surface residual stress and microhardness distribution for the three types of surface hardening, providing the engineering application for Inconel718 surface hardening.

2. Test

2.1 Materials

In the paper, the Inconel718 nickle-base super-alloy was adopted, mainly including (mass fraction %): Ni 52.60, Cr 19.27, Nb 4.93, Mo 2.96, Ti 1.10, Al 0.49, Mn 0.165, Si 0.145, Co 0.135, C 0.058, and Fe margin, with heat treatment process: solution treatment at 980ºC and heat preservation for 1h; AC double aging treatment from 720ºC (8h) to 620ºC (8h), and the main mechanical property: σ_s 1345.5MPa, σ_b 1585MPa, δ 16.25%, φ 30.1%.

2.2 Methods

Apply UDRP, LSP and SP for the polished cylindrical sample (φ 6mm×35mm). The process parameters for UDRP include ultrasonic frequency 27600, current 0.6A, static pressure 0.16MPa, spindle speed 180r/min, feed rate/load 0.1mm/r, and rolling twice; the parameters for LSP: ND Glass pulse laser, wave length 1064nm, pulse width 10ns, impulse frequency 10Hz, laser beam diameter 3mm, and pulse laser energy 4J; the parameters for LP: intensity of shot peening 0.13A, shot peening pressure 0.23b, shot time 160s and coverage 100%. The OLS4100 laser confocal scanning microscope was adopted to observe the surface morphology of sample, and measure surface roughness. Make electrolytic polishing (5vt% perchloric acid+95vt% ethyl alcohol, 20V, 0.4A, 30s) after water-sanding the sample by EBSD to 7000W, and then scan the steps and range respectively as 1μm and 500μm×240μm. Finally apply Channel 5 software to analyze the EBSD results. Use X-ray stress analyzer to measure the distribution of residual compressive stress against the layer depth, with the specific test parameters: Mn Kα target material, (311) crystal face, diffraction angle 151°, force constant -349MPa, collimator diameter 1mm, ψ = 0, 45°in sin2ψ, scan range 158°-143°, scan step 0.05°, count time 1s, voltage 18kV, current 4mA.

For micro-hardness, take the intersecting surface of the sample, sand finish and then polish it, and adopt the ultra-micro dynamic hardness device to measure the surface micro-hardness with measuring force 196mN and load holding for 10s.

3. Test results and discussion

3.1 Surface roughness and morphology

It was measured that the surface roughness of WS was 0.222μm, while that of UDRP, LSP and SP surface was 0.0134, 0.24 and 0.595μm respectively. The surface roughness after SP was increased obviously, about 2.68 times of WS; the surface roughness after UDRP decreased a little but it almost made no change after LSP. Fig.1 shows the 3D topography of the four surface states. Due to the arc-surface rather than flat surface, there emerged a big difference between the four surface states in the topography, but the actual surface roughness varied little. The 3D topography also shows that SP surface has obvious shot marks fluctuation, while there are no obvious height changes in WS, UDRP and LSP, resulted from the lower roughness values of these three types and smaller multiple for the 3D profilometry. But the 2D topography in Fig.2 indicates that despite the polishing treatment, the WS surface still was left with some cutting marks, UDRP surface with weaker marks, and on LSP surface, besides the original machining marks, there also left more obvious marks by LSP, therefore, after UDRP, LSP and SP surface hardening for Inconel718 super-alloy, the surface roughness by UDRP is the least, LSP slightly more than WS, and SP surface roughness increased the most.

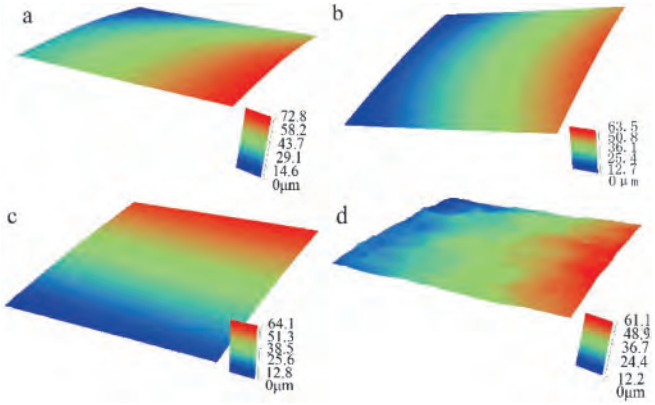

Fig.1 3D surface topographies of WS (a), UDRP (b), LSP (c) and SP (d)

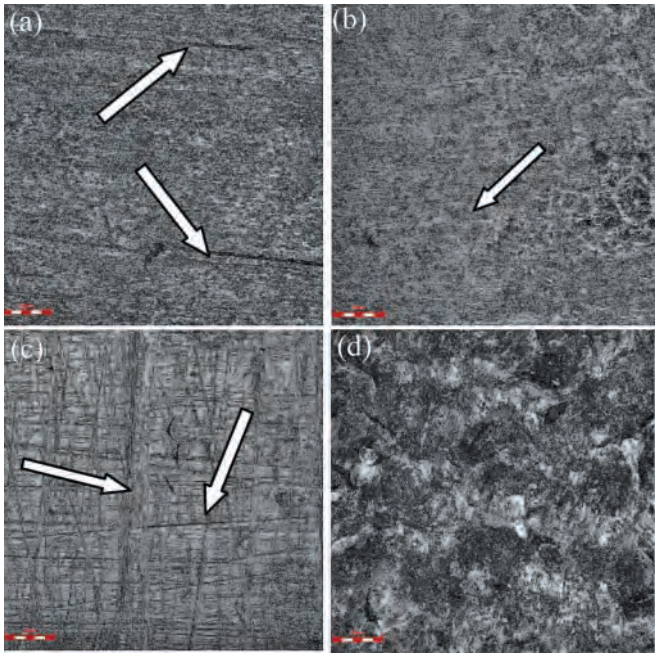

Fig.2 2D surface topographies of WS (a), UDRP (b), LSP (c) and SP (d)

3.2 Deformation microstructure analysis of EBSD

Fig.3 depicts the EBSD crystal grain orientation of the intersection surface in the four samples, and yellow, green and red crystal boundary represents low-angle boundary (mis-orientation less than 15°), high-angle boundary (mis-orientation more than 15°), and twin boundaries (mis-orientation of <111> shaft: about 60°). The bar graph of crystal mis-orientation statistic distribution in Fig.4 shows, compared to the un-hardened surface, the low-angle boundary of the four surface states occupied higher proportion, e.g. in the AISI304 stainless[20] surface

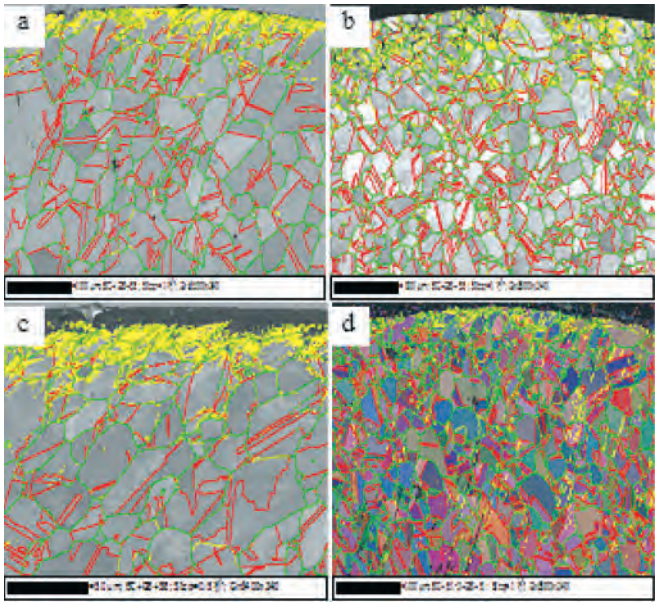

Fig.3 Grain orientation map of WS (a), UDRP (b), LSP (c) and SP (d)

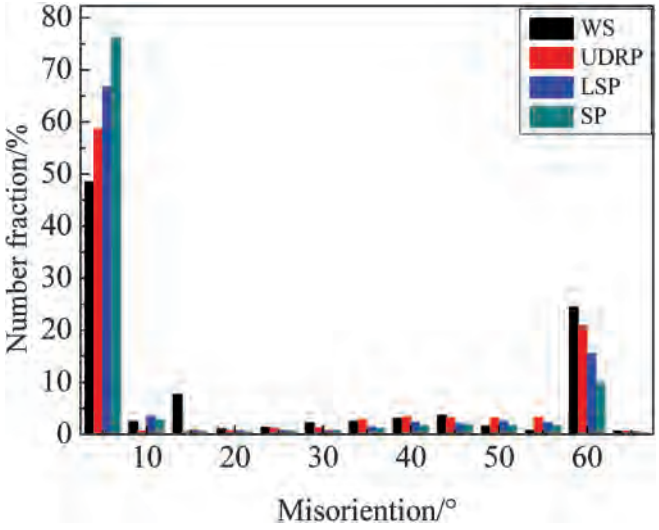

Fig.4 Misorientation angle distribution histograms

mechanical attrition treatment (SMAT) and FGH4097 powder metallurgy super-alloy shot peening hardening, because the plastic deformation might happen in the surface hardening process, then causing lots of dislocation and form the dislocation boundary. The low-angle boundary of the three surface hardening types takes up higher proportion at different growth rate: SP>LSP>UDRP.

In EBSD strain contour map, with crystalline grain as unit, take the maximum value of mis-orientation between any two points in the grains, determine certain colour, and then follow the given equivalent radius to the surrounding grain, to gain the micro-cell strain degree and distribution [21]. Hence, the strain contour map of different surface states in Fig.5 depicts that, compared to un-hardened surface, the micro-cell strain increased after the three surface hardenings, having a larger influence range. The LSP, as one non-shot shock using the high pressure blasting plasma to blast the material surface at high speed, has less impact on layer depth than the shot shock, but present more balanced shock in sub-surface, therefore, the LSP microcell strain layer is shallower than UDRP and SP (in Fig 5.b, 5.c and 5.d), but with balanced and continuous strain distribution in sub-surface. For the UDRP and SP with shot shocks, even with the ultrasonic burnishing twice and 100% shot peening coverage, there still existed blue zero strain zone on the sample surfaces, indicating that the shot shock was difficult to ensure 100% coverage, and it is necessary to further increase the UDRP rolling times, SP coverage rate and reduce the UDRP rotation and feed rate. Due to the different interaction between the shots and sample surfaces, UDRP and SP varies in the micro-cell strain distribution; the comparison between Fig 5.b and Fig 5.d shows that within the range 0-100μm from the surface, SP micro-cell strain degree is higher than UDRP, while within the range 100-240μm from the surface, UDRP strain degree higher than SP, meaning that within the range 0-240μm, the distribution gradient of UDRP micro-cell strain against layer depth is less than SP.

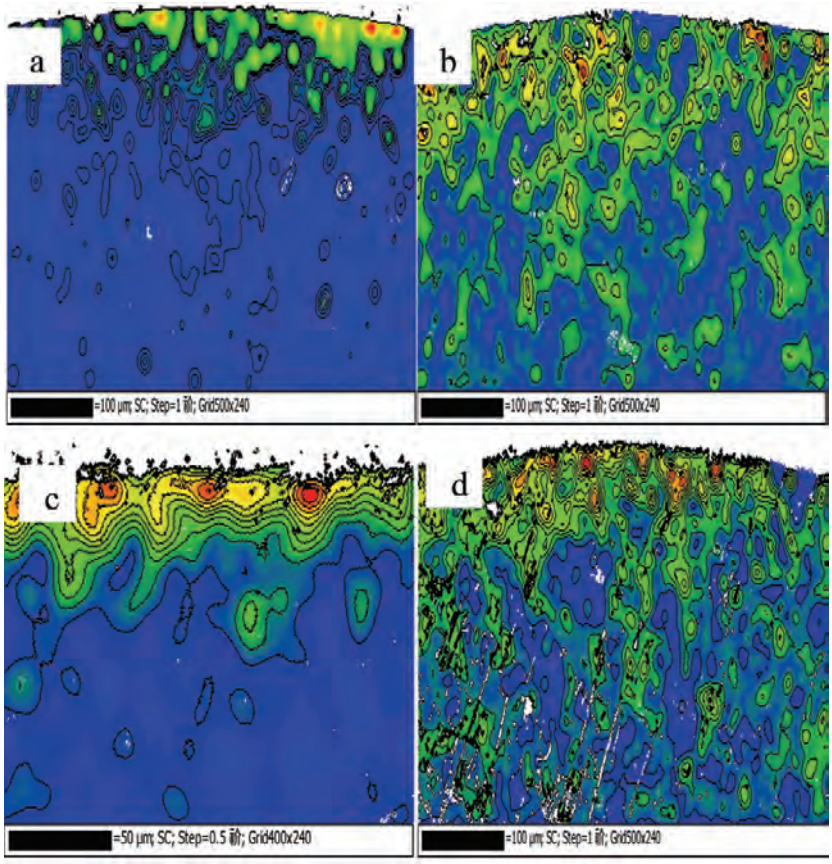

Fig.5 EBSD strain contour map of WS (a), UDRP (b), LSP (c) and SP (d)

3.3 Residual stress

Fig.6 depicts the distribution curve of residual stress against layer depth in the four different surface states for Inconel718. It was found in Fig.6 that the residual compressive stress of un-hardened surface for Inconel718 alloy was about 350MPa, which decreased with depth increasing with about 40μm layer depth of residual compressive stress. After applying the three hardening methods UDRP, LSP and SP for Inconel718, the residual compressive stress changed in the same trend as un-hardened surface, where the UDRP surface residual compressive stress was about 650MPa with layer depth about 350μm; the compressive stress of LSP surface about 900MPa with layer depth 350μm; that of SP is about 900MPa with layer depth 100μm; the results above were almost the same as the research in literature [4], but different from the literature [2] about the residual stress in hook form, which might be the reason that steel shot + glass shot was applied to the sample in literature [2]. Among these three hardening methods, the maximum residual compressive stress of LSP and SP is higher than UDRP, but with layer depth UDRP>SP>LSP.

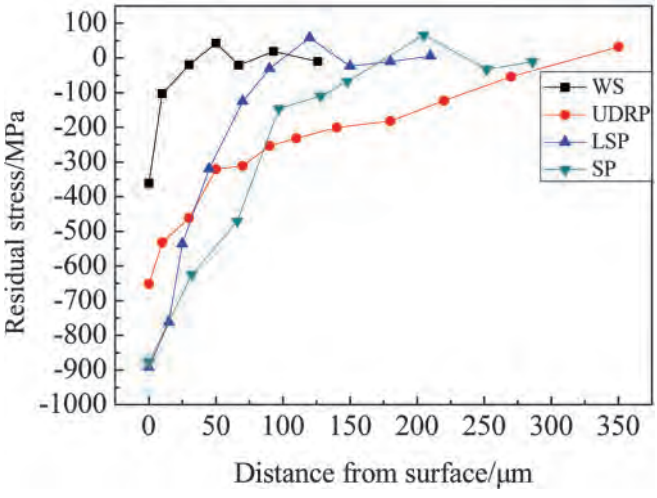

Fig.6 Residual stress curve

3.4 Micro-hardness

Fig.7 depicts the distribution curve of micro-hardness against the layer depth for the four surface states of Inconel 718, showing that the micro-hardness of Inconel718 alloy matrix was about 525DHV, and the micro-hardness of un-hardened surface was about 575 DHV, higher than alloy matrix because of its mechanical strain hardening effect, but with layer depth about 20μm. After UDRP, LSP and SP surface hardening, the surface micro-hardness all increased to some extent, where the LSP increased the most, about 725 DHV, and UDPR and SP about 650DHV, with the surface micro-hardness of SP was somewhat higher than UDRP; the hardened depth UDRP>SP LSP. It tallies with the previously-observed micro-cell strain and distribution change rule in EBSD, indicating that the change rule of micro-hardness is related to its micro-cell strain degree and the distribution change rule.

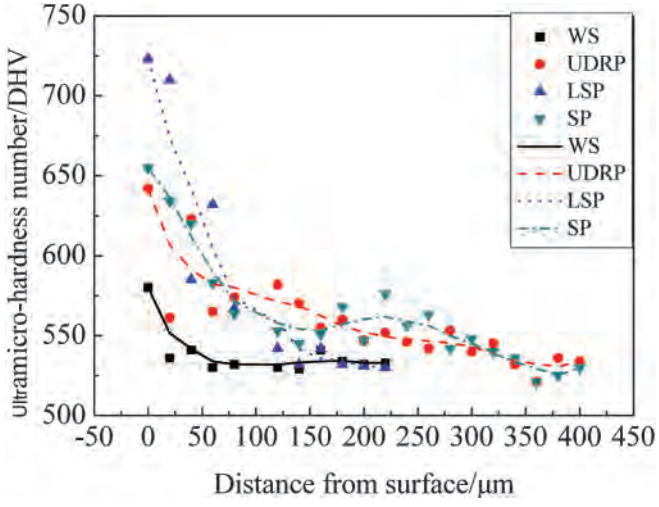

Fig.7 The curves of ultromicro-hardness in the surface layer

4. Conclusion

(1) Compared to un-hardened surface, the UDRP surface roughness decreases, and the LSP and SP surface roughness increases, where SP has the highest surface roughness. UDRP hardening can improve the sample surface quality.

(2) Among these three surface hardening methods, LSP presents the most balanced micro-cell strain distribution in Inconel718, but with the least layer depth; UDRP and SP has similar layer depth, but with micro-cell strain gradient lower than LSP.

(3) The residual compressive stress of the three surface hardening methods changes the same with the unhardened surface, and the residual compressive stress decreases with the layer depth increasing; for the surface residual compressive strength, LSP about 900MPa, close to that of SP, and UDRP about 650MPa, the least; for layer depth of residual compressive stress, UDRP>SP>LSP.

(4) The micro-hardness is related to micro-cell strain degree with surface microhardness LSP>SP>UDRP and hardened depth UDRP>SP LSP.

Acknowledgment

This study was financially supported by the Natural Science Foundation of Guizhou Province, China (Grantnos [2014] 2003 and [2014] 6012).

References

1. China Superalloys Handbook, 3rd ed., High temperature materials branch of China metal institute Co., China Zhijian Publishing House, Standards Press of China, BJ, 2012, pp.689-690.
2. Tang, Z. G. (2006): "Residual stress field and stress relaxation in shot peened Inconel 718," *Journal of Yanshan University*, vol. 30, no 6, pp. 503-506, 2006.
3. Song, Y. G. (2010): "Investigation of microstructure of GH4169 alloy surface layer sfter shot peening," *Heat Treatment of Metals*, vol.35, no.9, pp. 94-97, 2010.
4. Wang, X. (2015): "Effects of shot peening on high-temperature lpw-cycle fatigue property of GH4169 superalloy with hole structure," *China Surface Engineering*, vol. 28, no. 6, pp. 7-12, 2015.
5. Feng, S. (2008): "Research on surface nanocrystallization induced by high energy shot peening GH4169 superalloy," *New thch. & new process*, no. 6, pp. 88-90, 2008.
6. Shao, J. (2015): "Research on the thermal calculation method of high strength aluminium strip rolling based on finite different method," *Inter. J. of Heat and Tech.*, vol.33, no. 1, pp. 91-98, 2015.
7. Boutra, A. (2017): "Free convection enhancement within a nanofluid' filled enclousure with square heaters," *Inter. J. of Heat and Tech.*, vol.35, no. 1, pp:447-458, 2017.
8. Feng, S. (2008): "Research on high temperature oxidization property of GH4169 and 1Cr17 with nano-sized surface," M.S. thesis, Mater. Sci. Pro. Dept., Dalian Jiaotong Univ., DL. China, 2008.
9. Wu, S. T. (2015): "Preparation ans characterization of Fe_2O_3 micro-nano materials," *Inter. J. of Heat and Tech.*, vol. 33, no. 2, pp. 57-62, 2015.
10. Cheng, S. P. (2017): "Effect of high energy shot peening on the microstructure and properties of GH4169 alloy," M.S. thesis,Mater. Eng. Dept.,NC. HK. Univ., NC. China, 2017.
11. Sandá, A. (2011): "Surface state of Inconel 718 ultrasonic shot peened: Effect of processing time, material and quantity of shot balls and distance from radiating surface to sample," *Mater. & Design*, Vol. 32, no.4, pp. 2213-2220, 2011.
12. Pang, Y. H. (2012): "Experimental investigation and finite element analysis on residual stress field in LSP inconel 718," *J. of Fuzhou Univ.*, vol.40, no.3, pp. 370-375, 2012.
13. Teng, H. S. (2014): "Study on stress-strain field and microstructure of inconel718 alloy by laser surface treatment," M.S. thesis, Mater Eng. Dept., Yan Shan Univ., QHD, China, 2014.
14. Zhou, J. Z. (2015): "Effect of different process temperatures om residual stress and nano-hardness of warm laser peened IN718 superalloy," *Chin. J. of Lasers*,vol.42, no. 7, pp: 85-92, 2015.
15. Zhou, J. Z. (2016): "Thermal relaxation behaviour of residual stress in warm laser peened Inconel718 superalloy," *Rare Metal Mater. And Eng.*, vol. 45, no. 6, pp: 1509-1514, 2016.
16. Doo, K. H. (2014): "Rotary bending fatigue and seizure characterisitics of inconel718 alloy fager ultrosonic nanocrystal surface modification (UNSM)eatment," 8th International Symposium on Superalloy 718 and Derivatives, 2014.
17. Kim, J. (2015): "Rotary bending fatigue properties of Inconel 718 alloys by ultrasonic nanocrystal surface modification technique," *J. Eng. no.1*, pp:1-5, 2015.
18. He, J. (2017): "Effect of surface ultrasonic rolling process parameters on fatigue life Inconel718," *Hot Working Tech.*, vol. 46, no. 10, pp: 108-111, 2017.
19. Gill, A. (2013): "Comparison of mechanisms of advanced mechanical surface treatments in nickel-based superalloy," *MSE:A, no.576*, pp. 346-355, 2013.
20. Liu, S. (2014): "A research on the microstructure evolution of austenite stainless steel by surface mechanical attrition treatment," *MSE:A, no.617*, pp. 127-138, 2014.
21. Liu, T. G. (2011): "Application of EBSD to analyzing low strain level microsturcture," *J. of Chin. Ele. Microscope Society*, vol. 30, no. 4-5, pp: 408-413, 2011.